Stephanie Greenish
Vincent Hayward
hayward@cim.mcgill.ca
Center for Intelligent Machines
McGill University
3480 University Street
Montréal, Qc, Canada H3A 2A7

Vanessa Chial
Allison Okamura
Department of Mechanical Engineering
The Johns Hopkins University
Baltimore, MD

Thomas Steffen
Orthopaedic Research Laboratory
Royal Victoria Hospital
Montréal, Québec, Canada

Measurement, Analysis, and Display of Haptic Signals During Surgical Cutting

Abstract

The forces experienced while surgically cutting anatomical tissues from a sheep and two rats were investigated for three scissor types. Data were collected in situ using instrumented Mayo, Metzenbaum, and Iris scissors immediately after death to minimize postmortem effects. The force-position relationship, the frequency components present in the signal, the significance of the cutting rate, and other invariant properties were investigated after segmentation of the data into distinct task phases. Measurements were found to be independent of the cutting speed for Mayo and Metzenbaum scissors, but the results for Iris scissors were inconclusive. Sensitivity to cutting tissues longitudinally or transversely depended on both the tissue and on the scissor type. Data from cutting three tissues (rat skin, liver, and tendon) with Metzenbaum scissors as well as blank runs were processed and displayed as haptic recordings through a custom-designed haptic interface. Experiments demonstrated that human subjects could identify tissues with similar accuracy when performing a real or simulated cutting task. The use of haptic recordings to generate the simulations was simple and efficient, but it lacked flexibility because only the information obtained during data acquisition could be displayed. Future experiments should account for the user grip, tissue thickness, tissue moisture content, hand orientation, and innate scissor dynamics. A database of the collected signals has been created on the Internet for public use at www.cim.mcgill.ca/~haptic/tissue/data.html.

1 Introduction

Virtual surgery holds many promises. It could be used to train surgeons in virtual environments without the need for cadavers. It could also allow experienced surgeons to practice new techniques, accommodate a "brushing-up" for rarely used techniques, and help plan an operation. Furthermore, it could enable the planning and evaluation of completely new surgical techniques and eventually serve as a prediction method for their outcome. (Kuppersmith, Johnston, Jones, & Herman, 1996).

Realism in a simulation is increased with the addition of each sensorial modality, but, at present, most systems lack a good integration of tactile feedback, in part due to hardware limitations. Very few instruments and operating conditions can be reproduced. Other limitations arise from the lack of computational models representing the mechanical phenomena underlying haptic interaction. Yet other limitations come from the lack of knowledge of the factors that contribute to realism in the simulation of haptic tasks.

Presence, *Vol. 11, No. 6, December 2002,* 626–651

Current simulations in surgical procedures are mostly, if not completely, visual in the cutting aspect. This work is motivated by the need for haptic displays not to be limited to "poking" and "pulling," but also to address such basic tasks as cutting with scissors. Virtual simulations, when carefully constructed from measured data and conveyed via adequate devices, could actually be more realistic than cadaver tissues, which have significantly different mechanical properties than do living tissues. These simulations will also be more practical than physical phantoms, which cannot be reused. In addition, the need to sacrifice animals for surgical training or dissection is reduced.

This paper investigates the forces experienced by a surgeon while cutting different tissues. The data were analyzed to answer the following questions. Is there a quantifiable difference when cutting different tissues? Is the force measured invariant with the velocity? Are there any invariant properties of the tissues or of the scissors that can be determined? Is it possible to design computer-controlled scissors that can pass a test of realism? Can subjects identify tissues by feel alone, and how does this performance degrade when cutting virtual tissues?

2 Previous Work

One of the earliest efforts in virtual surgery was the Green Telepresence Surgery System, which was developed at SRI International and included a surgeon's console and a remote unit that performs operations on a patient (Green, Jensen, Hill, & Shah, 1993). SRI has also developed the MEDFAST system, a battlefield version to provide surgical services in dangerous environments (Satava, 1996), wherein a surgeon operates in a virtual space at a console and the motions are translated by a slave robot to a remote patient. Hunter, Jones, Sagar, Lafontaine, & Hunter (1995) pioneered this concept for microsurgery. Baumann, Maeder, Glauser, and Clavel (1998) described a force-reflecting system capable of addressing laparoscopic procedures, as did Basdogan, Ho, Srinivasan, Small, and Dawson (1998).

Other research in the development of surgical simulators was the work of Delp, Rosen, and associates of MusculoGraphics and MedicalMedia, who developed the anatomical rendering, tissue interactions, and surgical instruments for a specific surgical instance: a gunshot wound in the thigh. Delp, Loan, Basdogan, and Rosen (1997) presented a three-dimensional, interactive computer model of the human thigh, which was constructed from data provided by the Visible Human Project (Ackerman, 1994). Similarly, Merrill, Higgins, and colleagues of High Techsplanations developed the anatomic rendering, the tissue interactions, and surgical instrumentation for a shattered kidney (Satava & Jones, 1997). Eisler of Mission Research Corp. worked in tissue damage as a result of a ballistic wound for which Cuschieri from the University of Dundee supplied basic tissue properties (Satava & Jones, 1997).

Several researchers built systems to display "internal forces" between the thumb and finger for surgical tasks. Hannaford and colleagues (Hannaford et al., 1998; MacFarlane, Rosen, Hannaford, Pellegrini, & Sinanan, 1999; Rosen, Hannaford, MacFarlane, & Sinanan, 1999) designed a force feedback endoscopic grasper that displayed forces measured by a teleoperated grasper to the user's thumb and index fingers through a master haptic device. They demonstrated that subjects could discriminate between six different tissue types during teleoperated grasping using force feedback alone. Resolved-force haptic devices were used to display external cutting forces of a single blade in surgical procedures (Mahvash & Hayward, 2001; Biesler & Gross, 2000; Hirota, Tanaka, & Kaneko, 1999). In addition, cutting with scissors was modeled, without the display of internal cutting forces, by Picinbono, Delingette, and Ayache (2000) and Basdogan, Ho, and Srinivasan (1999). Other related works were concerned with the recording of the interaction of the jaws of a laparoscopic surgical instrument with tissues (Bicchi, Canepa, De Rossi, Iacconi, & Scilingo, 1996), with internal force feedback device transparency (Longnion, Rosen, Sinanan, & Hannaford, 2001), or with the puncture-force response of spleen and liver in animals (Carter, Frank, Davies, & Cuschieri, 2000). Several efforts are now directed at obtaining in vivo measurements of the mechanical properties of biological materials (Vuskovic, Kauer, Szekely,

& Reidy, 2002; Ottensmeyer & Salisbury, 2001; Brower et al., 2001).

The present study of using haptic recordings fits into a larger class of research devoted to the use of real-world measurements in haptic rendering. The most comprehensive system for acquiring data for reality-based modeling thus far is the Active Measurement Facility (ACME), built by Pai, Lang, Lloyd, and Woodham (2000). They have obtained reflectance, stiffness, texture, and sound data by probing objects, fit these data to analytical and empirical models, and generated realistic virtual environments (Richmond & Pai, 2000). MacLean (1996) has created realistic virtual environments using the concept of a "haptic camera" that captured haptic information about real environments. Other examples of empirical haptic models include work on friction by Richard, Cutkosky, and MacLean (1999) and vibrations by Okamura, Dennerlein, and Howe (1998) and Okamura, Hage, Dennerlein, and Cutkosky (2000).

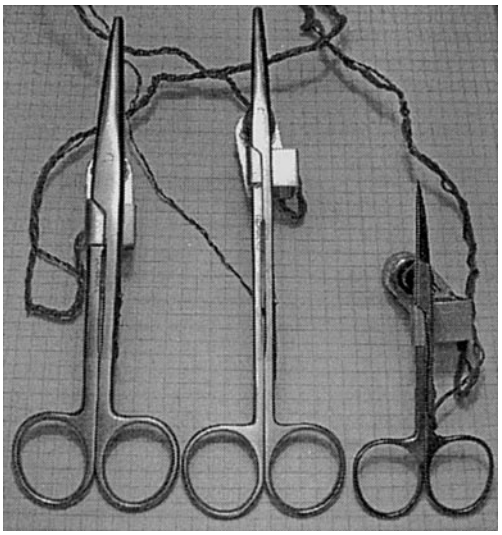

Figure 1. *The instruments used (from left to right: Mayo, Metzenbaum, and Iris, as in figure 5).*

3 Materials and Methods

Data were acquired with three instrumented surgical scissors: Mayo dissection scissors, Metzenbaum dissection scissors, and the Iris scissors. The last author provided general directions and professional expertise to prepare three separate animal experiments at the approved McGill University animal-care facilities. The data collected are from his hand and that of his students. All data collection was performed on animals that had been sacrificed for other research and in accordance with animal protection laws. Because they were planned sacrifices, it was possible to perform the experiments immediately after death, minimizing postmortem effects.

3.1 Instruments

Among the thousands of surgical instruments, there exist distinct classes of basic handle designs. A most common class is that of the scissor handles. For scissors, many variations exist in the handles and blades. The blades can have different lengths and breadths. They can have teeth or not, be curved or straight, and pointed or blunt. Furthermore, the blades can be sharp or dull, tight or loose depending on the joint screw, and each of these factors influences the "feel" of the scissor. For the scissor, the central aspect of the haptic experience results from closing them around a tissue region, and hence the scissor angle is the primary state variable.

It was learned that surgeons often prefer a curved tip, which allows more visibility of the work area. The instruments used for experimentation were a 7 in. (17.8 cm) Metzenbaum scissor with tungsten carbide inserts, a 6.75 in. (17.1 cm) Mayo scissor with tungsten carbide inserts, and a pair of 4.5 in (11.4 cm) Iris scissors (all with curved tips). Piling-Weck's gold-handled scissors were selected for their smooth and sturdy feel. (See figure 1.)

3.2 Tissues

The tissues compared were from a sheep and two rats. Tissues were selected because of their accessibility and relative abundance, but also because of their distinct properties: skin (abdominal region), the abdominal muscle wall, the liver, and the calcaneal (or Achilles) tendon. The three layers of the abdominal muscle wall

(oblique external, internal and transversal abdominal) were cut as one tissue. For the sheep experiments, muscle-rectus fascia was also cut because it was available in abundance in the fatty abdominal area of the sheep.

3.2.1 Tissue Preparation. For each run, a piece of tissue was prepared and isolated from the surrounding layers. This involved scraping away excess fascia to keep the thickness relatively constant and pulling the tissue out so that it was accessible. Care was taken to remove as much of the surrounding tissues; however, there is an inherent tradeoff between tissue preparation and time, and, hence, postmortem effects. Therefore, the thickness varied as an innate property and as a function of the amount of other tissues attached to the sample of interest. Hence, it was only feasible to use approximately even samples from run to run. This would not be a problem if the sample sizes were very large, but that could not be the case here. This brings up another issue, which is mentioned by Duck (1990). These experiments were performed on one sheep and two rats, which did not allow for an average between animal ages or sizes. The effect of the experimental limitations required to minimize the postmortem effects are further discussed in subsection 4.2.6.

3.2.2 Cutting Conditions. Skin and muscle tissues were tested in the longitudinal (L) and transversal (T) directions, which for the muscle was defined by the orientation of the contractile fibers and for the skin by the Langer lines. Cuts were made at two speeds selected by the physician: one designated as fast, and the other slow. Generally, slow corresponded to less than 15 deg./sec. and fast to greater than 15 deg./sec. More details are provided in subsection 4.5.

3.3 Instrumentation

The scissors were instrumented with strain gauges (Entran ESU-025-1000), and quarter-turn precision potentiometers (Midori CP-2UTX), so both displacement and force could be measured. An Analog Devices 3B Series signal conditioning unit was used with external bridge balancing. Half-bridge configurations were used for the Mayo and Metzenbaum scissors because one gauge was in compression and the other in extension on the scissor arm at the point of maximum bending. A quarter-bridge configuration was used for the space-limited Iris scissors. Bridge completion was provided with two dummy resistors (MicroMeasurement module MR1-10C-129). The signals from the potentiometers did not require conditioning. Identification of the mechanical transfer function of the scissors was conducted to determine an adequate sampling frequency. It was taken to be ten times the maximum bandwidth found, or 1 kHz. Twelve-bit analog-to-digital converters were used. A personal computer running QNX handled data acquisition of the force and position data. A graphical user interface was implemented to provide for simple operation in the field.

3.3.1 Calibration. The free body diagram for the scissor, assuming symmetrical loading, is presented in figure 2(a).

The static equilibrium conditions are

$$\sum F_x = R_x + F_1 \sin\theta - F_2 - F_{ct} \cos\theta + F_{cb} \sin\theta = 0 \quad (1)$$

$$\sum F_y = R_y + F_1 \cos\theta - F_{ct} \sin\theta - F_{cb} \cos\theta = 0 \quad (2)$$

$$\sum F_z = R_z + F_3 - F_{cz} = 0 \quad (3)$$

$$\sum M_{oz} = M_f + F_1 L_1 + F_2 L_1 \sin\theta + F_{cb} L_2 = 0 \quad (4)$$

$$\sum M_{oy} = F_3 L_1 - F_{cz} L_2 = 0 \quad (5)$$

The force F_2 applied by the surgeon to push against the scissors was assumed to be small compared to F_1, the force to close the scissors, and hence was neglected. F_2 may become important in unusual cases, such as when the object being cut is very hard (cutting bone) or very thin (cutting a sheet). Assuming small angles ($\theta < 30°$), equation (4) reduces to

$$\sum M_{oz} \approx M_f + F_1 L_1 + F_{cb} L_2 = 0. \quad (6)$$

Neglecting friction M_f in the joint, equation (6) reduces to

$$F_1 L_1 = F_{cb} L_2. \quad (7)$$

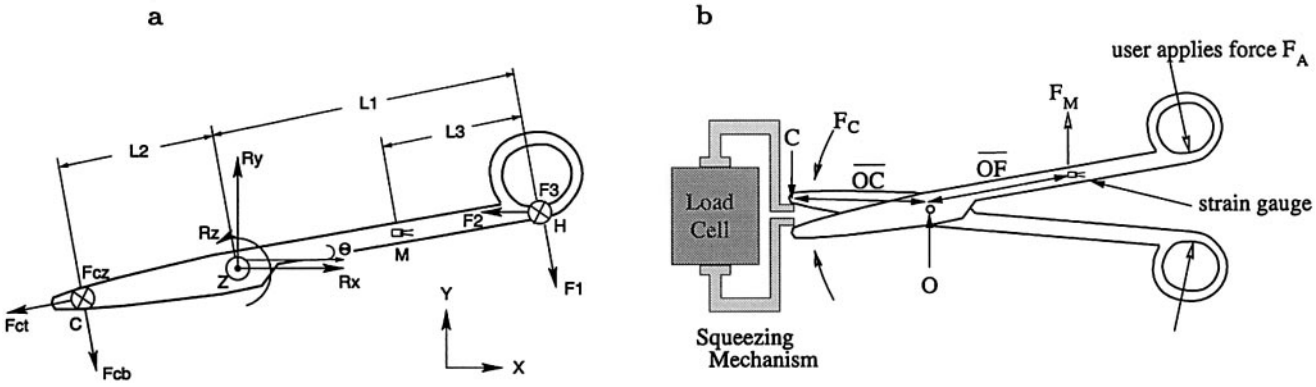

Figure 2. *(a) Free body diagram of scissors. (b) Setup used to calibrate scissors.*

This equation was used to convert the strain gauge readouts to a cutting force F_C measured in Newtons after calibration using the setup in figure 2 with a calibrated load cell (RDP Electrosense type E308).

Equation (7) is re-expressed as

$$F_M \overline{\mathrm{OF}} = k\, F_C \overline{\mathrm{OC}}, \tag{8}$$

where k is a constant characteristic of each instrument.

The linear correlation $r = \mathrm{SS}_{xy}/\sqrt{\mathrm{SS}_{xyxx}\mathrm{SS}_{xyyy}}$ was used as a goodness-of-fit measure (Mann, 1998). The r's were found to be 1.00 for the Mayo, 1.00 for the Metzenbaum, and 0.96 for the Iris. The forces compared in all subsequent discussion are resolved at the cutting point.

3.4 Data Segmentation

The data were segmented with a velocity zero-crossing method: first by selecting the data points in the velocity vector smaller than some ε (typically $\varepsilon < 0.05$), and then eliminating those that are closer than γ data points apart (typically $\gamma > 100$), to ignore segments of steady position. It was found that there are consistently four distinct phases in cutting: (i) opening the scissor, (ii) resting, (iii) closing the scissor, and (iv) resting before opening again. (See figure 3(a) and 3(b).) Negative forces indicate scissor opening.

4 Results and Discussion

4.1 Scissor Differences and Invariants

In situ measurements prevented us from controlling many variables. To partially compensate for this, several controlled runs were performed cutting paper. These runs are presented in figure 4 for the cutting of two and four sheets of 20 lb. standard printer paper. Each graph is composed of more than ten cuts overlapped.

4.1.1 Breakthrough Angle. In figures 4(a) and 4(b), as the Mayo scissor cuts through the paper, the F_C increased until close to 5°, after which the force dropped off. This dropoff for the Metzenbaum scissors, figures 4(c) and 4(d), was closer to 8°, whereas this dropoff did not seem to exist for the Iris scissors until the scissors had fully closed and the cut was finished (figures 4(e) and 4(f)). This was related to the geometry of the blades: both the Mayo and Metzenbaum have blunt tips, and therefore the scissor blades slide past each other before the handles are closed. The Iris scissors have pointed tips so their blades close when the handles collide. This is shown pictorially in figure 5(b), the Metzenbaum blades just closed at the 8° opening angle. The Mayo scissors in figure 5(a) must close a bit more before the blades completely close against one

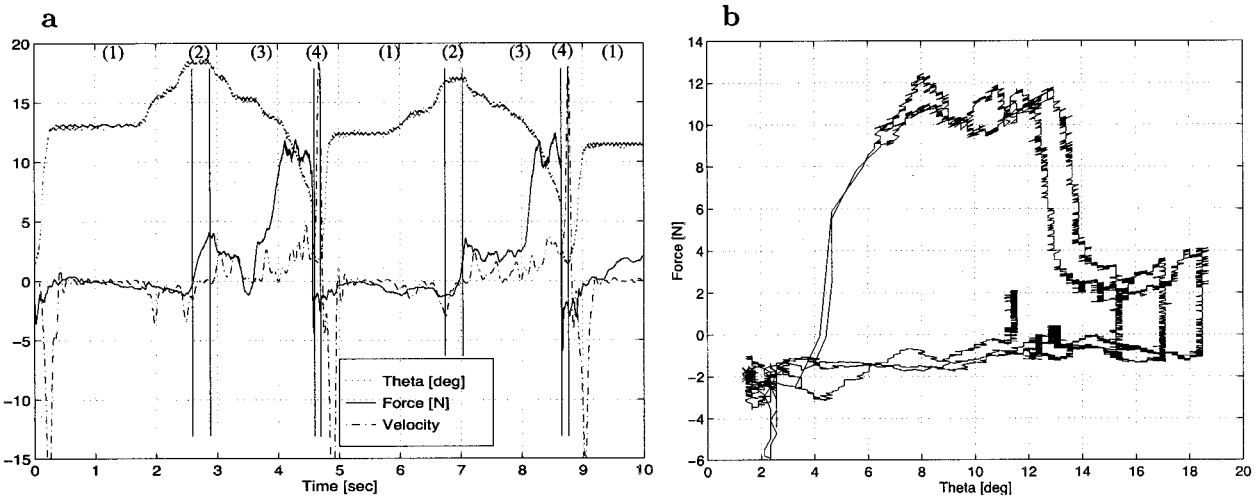

Figure 3. *Curves to analyze force versus position relationship. (a). Force, velocity, and position θ data for a typical cut with the Metzenbaum dissecting scissors. Phase (1): opening. Phase (2): resting before closing. Phase (3): closing. Phase (4): resting before opening. (b). Force versus theta position data for a typical cut with the Metzenbaum dissecting scissors. The vertical data segments are explained in subsection 4.2.3.*

another, which corresponds to the 5 deg. mentioned earlier.

Also depicted in figure 5 are the differences in the contact surface areas of the two blades for the different scissor types at the two angles, 20 deg. and 8 deg. These differences are seen in "blanks" that corresponded to opening and closing the scissors in thin air. It was found that the Mayo scissors had the tightest joint screw, which is seen in the blank runs (figure 6). The tightness of the screw, the sharpness of the blade edges, and the flexibility of the arms vary considerably from scissors to scissors.

4.1.2 Scissor Characteristic Slope. One might expect that the force required to cut four sheets of paper as shown in figures 4(b), (d), and (f) would require twice as much force as cutting two sheets of paper, as in figures 4(a), (c), and (e). As the data show, this is not so. The ratio was approximately 1.6 for the Mayo, 2.5 for the Metzenbaum, and 1.4 for the Iris.

There was, however, a consistent increase in the F_C as the scissor closes. Moreover, the slope of the θ-F_C curve are related to the maximum of the F_C. For example, the slopes of the curves to cut two sheets of paper for the Mayo and Metzenbaum scissors were -0.48 and -0.33 N/deg., respectively (figures 4(a) and (c)). The corresponding maximum F_C are 12 N and 10 N. The slopes of the curves for cutting four sheets of paper were -0.56 and -0.75 N/deg., and the maximum F_C are 20 N and 25 N for the Mayo and Metzenbaum (figures 4(b) and (d)). Therefore, the scissors with the largest maximum F_C, the Metzenbaum, had the steepest slope.

4.1.3 Reversals. It is important to recall how an experienced surgeon actually uses surgical scissors, compared to a novice. The surgeon rarely closes the scissors completely. Once the sensation of having completely cut through a tissue is reached, the scissors are opened again. This provides greater control. A surgeon will not typically use scissors opened by more than 20° to make a cut because this results in reduced control while cutting and in the possibility of tissue sliding between the blades. Instead of making one large cut, many small cuts are made. The only time the scissor is used wide open is when it is used to spread tissues apart, as it is used during tissue preparation.

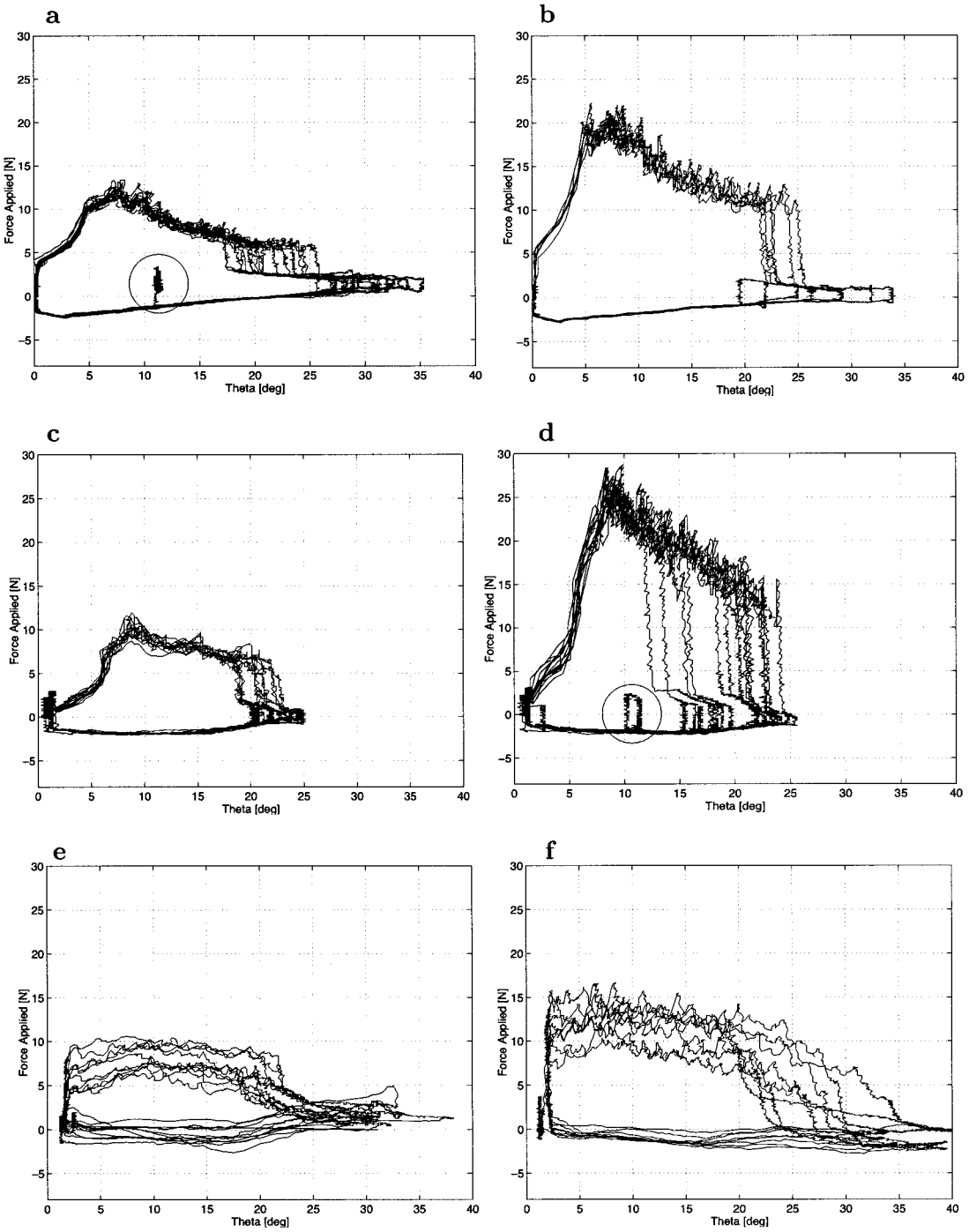

Figure 4. *Cutting of printer paper with Mayo, (a) two and (b) four sheets; with Metzenbaum (c) two and (d) four sheets, and with Iris scissors (e) two and (f) four sheets (student data).*

Although the angle at which the surgeon stops closing or opening varies, the behavior of the F_C between the endpoints was fairly constant. The beginning and the end of a cut were similar in that they both involved a rapid change in the F_C, but in opposite directions. At the end of a close, the force

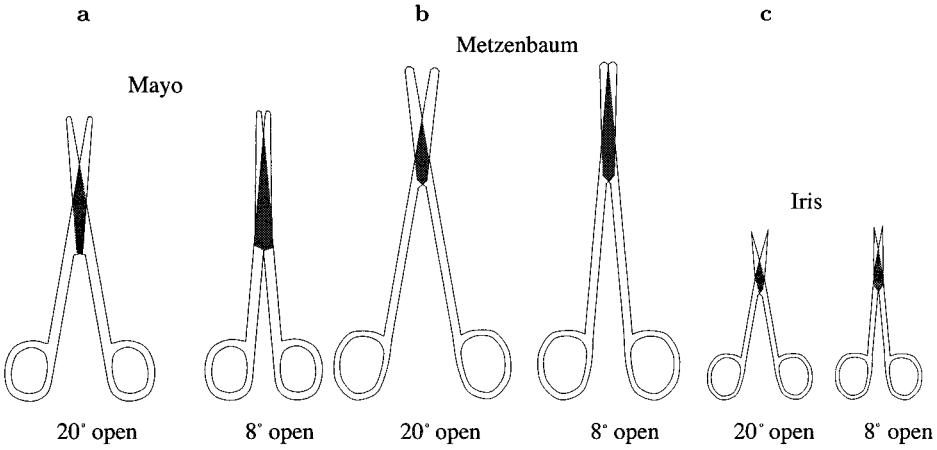

Figure 5. *Different overlap areas for different scissors blade types at same angles θ.*

dropped off quickly and at the beginning of a cut, the force rose quickly.

4.2 Tissue Differences

The tissues compared were from a sheep and two rats. Calling $F_C(\theta)$ the cutting force recorded as a function of θ, $\bar{F}_C(\theta)$ is the average force over several runs. The maximum of the average cutting force over all θ's, ${}^{\mathrm{m}}\bar{F}_C$, is then found and presented first to establish general trends. See table 1. The missing values are a result of experimental limitations.

4.2.1 Maximum Average Force. Looking first at the Mayo and Metzenbaum sections, the sheep tissues generally required more force to cut than did the rat tissues. This agreed with our expectation. The tendon was the only tissue that did not change dramatically in the ${}^{\mathrm{m}}\bar{F}_C$ required between sheep and rat. This was explained by the fact that, because the sheep Achilles tendon was massive, it was necessary to split it and cut only the number of strands that could reasonably be cut by the scissors. This resulted in a bundle close to the size of the rat Achilles tendon.

4.2.2 Comparing Blanks and Liver Cuts. One might expect these runs had the lowest ${}^{\mathrm{m}}\bar{F}_C$. This is true for the Iris scissors, but not for the Mayo and Metzenbaum scissors: the liver cut actually required less force than did the blank. For example, the average ${}^{\mathrm{m}}\bar{F}_C$ for the Mayo blank was close to 7.0 N, whereas for the rat liver it is 5.8/6.1 N (fast/slow). Similarly for the Metzenbaum, the blank had a ${}^{\mathrm{m}}\bar{F}_C$ of approximately 3.3 N, but the rat liver registered 1.6/2.5 N. On the other hand, for the Iris scissors, the rat liver required much more force to cut, approximately 10.2 to 10.7 N versus 5 N for the blank. The results for the Iris scissors are discussed first.

***F_C* of the Iris scissors:** All tissue cuts performed with the Iris scissors required more force than did the Mayo and Metzenbaum scissors. The shorter arm length had no bearing on the measurement, but the shorter blade length did. The Iris blade length was half that of the Metzenbaum blade. The forces were typically two to three times higher for the Iris than for the Metzenbaum scissors; therefore, factors must exist to account for these differences.

The Mayo and Metzenbaum scissor blades had tungsten carbide inserts that made their blade edges sharper and stronger than the Iris blades. Because the blades themselves are thicker for the Mayo and Metzenbaum scissors, they were less likely to bend laterally and disturb the cutting process. This does not explain, however, why the F_C for the Mayo and Metzenbaum scissors are lower than their respective blank cuts during the liver runs.

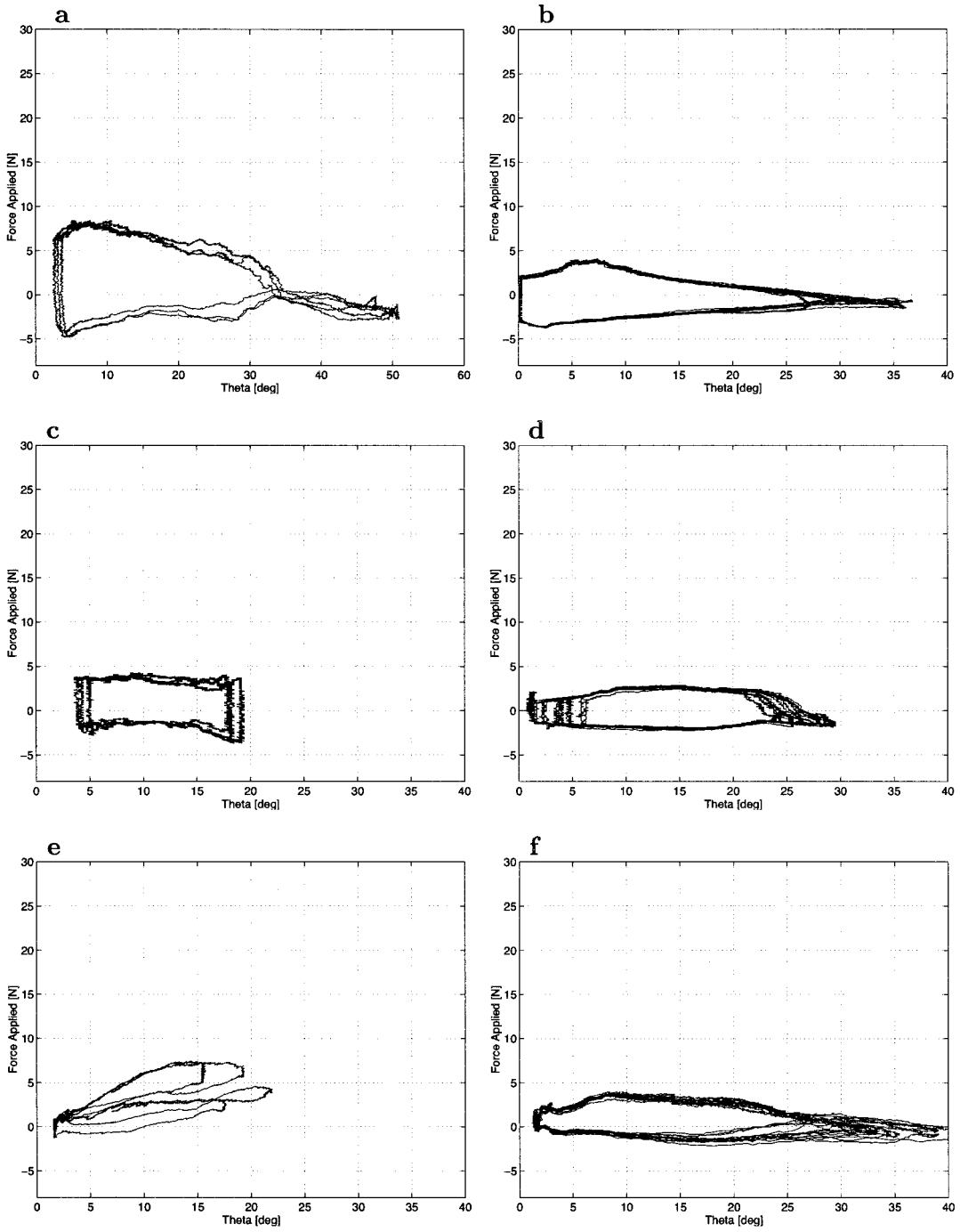

Figure 6. *Comparison of blank runs for Mayo scissors between (a) surgeon and (b) student, Metzenbaum scissors for (c) surgeon and (d) student, and Iris scissors (e) surgeon and (f) student.*

***F_C* of the Mayo and Metzenbaum scissors:** To explain why the Mayo and Metzenbaum liver runs registered a lower force than did the blank cuts, it was thought that blood was lubricating the scissors. However, this effect was not reproducible offsite: spraying the scissors with lubricant (WD-40) gave virtually the same $F_C(\theta)$ curves,

Table 1. *$^{m}\bar{F}_C$, the Maximum of the Average Applied Force at C for Different Tissue Types During Cuts by the Surgeon*

	Mayo		Metz		Iris	
Scissor	Closing	Opening	Closing	Opening	Closing	Opening
Blank (slow)	6.6	8.0	3.1	4.0	5.1	4.7
Blank (fast)	6.4	7.3	3.6	2.6	3.0	7.2
Tissue ↓ Animal →	Rat	Sheep	Rat	Sheep	Rat	Sheep
Skin (L, slow)	8.0	17.6	7.0	17.5	22.6	44.8
Skin (L, fast)	8.7	20.5	5.9	16.9	23.4	32.6
Skin (T, slow)	8.4	16.4	—	13.2	17.3	—
Skin (T, fast)	7.8	16.4	8.1	19.3	18.2	—
Muscle (slow)	10.2	—	—	—	16.6	—
Muscle (fast)	—	—	2.4	—	—	—
Muscle (L, fast)	—	5.8	—	—	—	14.0
Muscle (T, fast)	—	9.1	—	—	22.8	27.0
Liver (slow)	6.1	—	2.5	—	10.2	—
Liver (fast)	5.8	8.3	1.6	7.1	10.7	21.2
Fascia (slow)	—	7.8	—	—	—	12.5
Fascia (fast)	—	8.7	—	6.0	—	17.7
Tendon	22.8	24.6	30.5	—	—	—

which is consistent with the nature of friction. Lubrication in metal contacts is explained by hydrodynamic effects that play no role here, given the low velocities and the small contact areas involved.

Upon closer inspection, it was noticed that the blank runs performed by the student were different from the blank runs performed by the surgeon (figure 6). The surgeon registered a $^{m}\bar{F}_C$ of 8 N (table 1), which is shown graphically in figure 6(a); the student registered nearly half of that, 4.1 N (figure 6(b)). Similar results were obtained for the Metzenbaum scissors and for the Iris scissors: 4 N versus 2.9 N (figure 6(c) and (d)), 7.2 N versus 4.7 N (figure 6(e) and (f)). Therefore, the grip as well as the tissue and scissor types affected the force experienced. The grip used was probably a strong function of training and reveals that it is important to involve trained surgeons at these early stages of research.

4.2.3 Grip Change Effects. The grip affected the F_C as there was an increase or a decrease in the force when the scissor angle θ was not changing. In figure 4(d) at 11 deg. on the opening (lower) curve, there is a momentary change in the cutting direction. This caused a rapid increase in the force as a result of a brief closing of θ to 10 deg. (circled in figure). After this brief closing, the F_C again went down to the force level of the rest of the open curve, as the scissors were completely opened. Clearly, the short change in direction resulted in a momentary jump up to the corresponding blank closing curve (figure 6(d)), for the student blank Metzenbaum run. These rapid rises in F_C in the opening curve are also visible in data where there is no closing of the scissor but only a pause (figure 4(a) at 11 deg, circled in figure), due to static friction.

This indicates that there were at least two grips, an opening grip and a closing grip, interacting with differ-

ent regions of the rings. Because an increase in F_C occurred even when there was no closing action, there also seemed to be a grip change when stopping. This again implies that the grip had a strong influence on the forces read. As a note, it is also likely that a grip change caused the abrupt increase in F_C once the scissors had been completely opened, typically near 30 deg.

This grip effect may also explain the high variability experienced with the Iris scissors (figure 6(e)) wherein four cuts performed by the surgeon are plotted together. The high degree of variability was not seen in the student runs, however (figure 6(f), wherein more than ten cuts are plotted together.

4.2.4 Contact Between Object and Scissors.

Another observation can be made from figures 4(a) through (d). For all incident angles, the force level jumped to the same closing curve. The inner-most curve closed at around 15 deg. where the force level jumped from approximately −2 N to 1 N. When the scissors started closing, the force remained on the blank closing curve, then, near 12 deg., contact occurred with the tissue and force rose almost instantly to 20 N to meet the closing curve.

4.2.5 Longitudinal versus Transversal.

No clear relationship emerged from comparing the values for the longitudinal (along the body axis) and transversal cutting directions (table 1). Statistical analysis was therefore performed to determine whether there were significance in the data from sum of squares error analysis (SSE) (Mann, 1998). A significant difference between curves was taken as a difference in the SSE between the two directions, SSE_{L-T}, which was greater than the variability between the runs in any one direction, SSE_L or SSE_T. The average force curves in each direction were first calculated:

$$F_{D,\text{ave}}(\theta) = \frac{1}{N}\sum_{i=1}^{N} F_{D,i}(\theta), \tag{9}$$

where N is the number of runs and D is L or T. Then, variability in the two directions is calculated as

$$\text{SSE}_D = \sum_{i=1}^{N_D} (F_{D,\text{ave}}(\theta) - F_{D,i}(\theta))^2. \tag{10}$$

The sum square of the error could then be calculated as

$$\text{SSE}_{L-T} = \sum_{j=\min(\theta)}^{\max(\theta)} (F_{L,\text{ave}}(j) - F_{T,\text{ave}}(j))^2. \tag{11}$$

The results from this analysis are shown in table 2.

For the Mayo and Metzenbaum scissors, the differences between transversal and longitudinal cuts for both the rat and sheep skin were not significantly different. However, for the Iris scissors, the rat skin cut slowly registered as significantly different for the transversal and longitudinal directions. This can be due to the known variability of these scissors or to their higher sensitivity. Unfortunately, the fast skin cuts do not verify this result. From table 1, the ${}^{\text{m}}\bar{F}_C$ for the longitudinal direction is 23 N for the Iris scissors, and 17.8 N for the transversal skin direction. Because skin fibers are aligned with the transversal axis of the body, the longitudinal force should be higher. The more delicate Iris scissors may indeed be sensitive to the cutting directions of skin.

The two cutting directions were significantly different for the muscle cuts with both the Mayo and Iris scissors. Because muscle fibers are highly oriented strands, this is expected. These results are indeterminate for the Metzenbaum scissors because there were no data available for the slow muscle cuts. For the simulation of skin cutting with these scissors, it seems reasonable that the same model could be used for both cutting directions. However, a muscle cutting simulation should account for orientation.

4.2.6 Tissue Variability

Tissue Toughness: The differences between tissues of the same type are due to the fact that the properties of the layers changed from region to region in the animal. For example, the skin near the outside of the stomach area was tougher (and thicker) than the skin closer to the center. During experimentation, care was taken to use tissue from only a small region. However, there were many different experimental cutting conditions, which required a large quantity of uniform tissue.

Table 2. *Comparing Transversal and Longitudinal Directions for Cuts (Surgeon Data)*

Scissor	Tissue	Max (SSE_T, SSE_L)	SSE_{L-T}	Statistically different?
Mayo	Skin (sheep, slow)	3.1	1.5	N
	Skin (sheep, fast)	6.1	1.4	N
	Skin (rat, slow)	1.3	0.9	N
	Skin (rat, fast)	2.3	1.1	N
	Muscle (sheep)	0.6	2.4	Y
Metz	Skin (sheep, slow)	4.4	2.9	N
	Skin (sheep, fast)	6.1	1.4	N
	Skin (rat, fast)	3.5	2.2	N
Iris	Skin (rat, slow)	3.4	8.6	Y
	Skin (rat, fast)	4.6	4.1	N
	Muscle (sheep)	4.5	10.9	Y

Tissue Thickness and Preloading: To understand the effect of thickness and tissue strength on the cutting force, one must recall how tissue is cut. The applied force is a result of interaction with the tissue at and ahead of the cutting point. With closing, the amount of tissue deformed between the blades increases. This results in a gradual increase in the cutting force.

Although exact thickness control is not critical in this work where general trends are sought, it is an important factor to keep in mind for future experiments. A problem encountered was the folding over of the prepared tissues. The tissues had to be exposed, so they were held with forceps clamped near the corners. Initially, the assisting surgeon was holding the tissues just below the corners, and therefore the skin had no support in the middle. This resulted in the edge folding over on itself, resulting in a much larger F_C because the tissues were twice as thick. This effect can be seen in figure 7 where two runs were performed under the same conditions, longitudinal and fast, but give very different results. The F_C measured when the skin was folded over was nearly twice as much, approximately 12 N versus 6 N. Again, for reasons of time limitation, the possible effect of preload applied to the tissue could not be controlled as much as it should have been.

Unfortunately, this problem was not identified until part way through experimentation. Although most of the tests were repeated, similar tissue and time restrictions prevented all experiments from being repeated. This accounts for some of the values absent in table 1. The other missing data values include the tendon cuts for the Iris scissors. These experiments were not performed for fear of ruining the delicate Iris scissors with the tough tendon. As well, no liver experiments were run in slow speed for the sheep.

Effect of Sticking: Another variable was "stickiness" (as distinguished from friction) as a result of the blood drying on the blades. Because the animals were drained before experimentation, there was less blood in the tissues than when the animal is alive. Stickiness between the blades probably appears in the data as an increase in F_C. Spraying with saline solution was performed when deemed necessary, but it is possible that certain data files would require a slight correction. This error is not considered significant for the determination of general trends.

Summary: Overall, an accurate description of the tissues and experimental conditions is required for an exact force measure of one tissue type. It is not sufficient to simply specify "skin" or "fascia." The thickness of

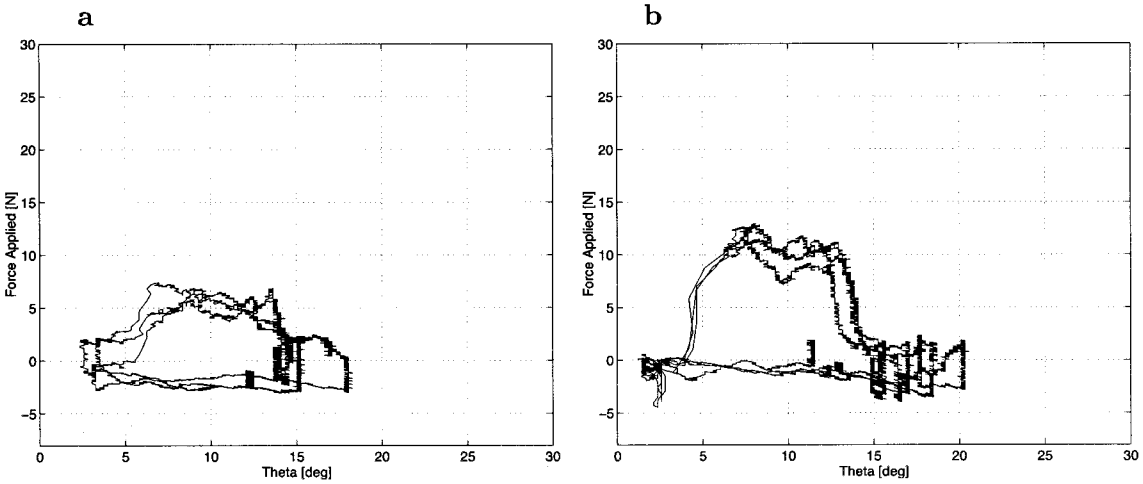

Figure 7. *The effect of having the tissue layer folded over. Both curves are for the fast, longitudinal cutting of rat skin with the Metzenbaum scissors where the skin is (a) normal and (b) folded.*

the tissue and moisture content play an equally important role in the resistance of the tissue and therefore should be measured. As well, future experiments should include more exacting tissue preparation and larger sample sizes.

4.3 Frequency Analysis

The power spectral density (PSD) of the force signal was obtained for the four task phases described in subsection 3.4. The signals have little high-frequency components for the four phases for each of the three scissors. The magnitude of the PSD response (in dB) was the highest for phase 3, or closing the scissors. For all of the tissue types (skin, liver, tendon, fascia), most of the frequency components are below 4–5 Hz, with a peak typically between 1.0–3.9 Hz. Figures comparing the power spectral density curves for the three scissors have been included for the cutting of sheep skin slowly. (See figure 8.) It is likely that the 1.0–3.9 Hz components were a property of the tissue being cut. From a modeling point of view, this suggests that only low-frequency signals need to be reproduced for realism. Furthermore, there must be differences other than the range of the frequency components to explain why the cuts for different tissues feel different.

4.4 Comparative Analysis

It is useful to compare some tissue-cutting curves as in figure 9 along with table 1. Looking first at the blank and liver cuts, the closing curves for these runs are relatively smooth, especially compared to the cuts for the muscle and skin. Comparing the muscle run to the blank, the differences are seen in the magnitude of the force during the closing phase, as well as in the bumpiness, or texture, of the muscle cut. The maximum of the average force curve ${}^{\mathrm{m}}\bar{F}_C$ for the blank cuts was around 6 N versus 9 N for the muscle. Whereas the skin cuts showed a similar behavior, the force magnitude difference was much less pronounced when compared to the blank run (reaching as low as 6 N).

Given the small change in ${}^{\mathrm{m}}\bar{F}_C$ for skin and liver runs as compared to blank runs, it was also possible to infer that, for these tissues cut with Mayo scissors, the tactile sensation was due to irregularities. This was opposite for the tendon, however, for which all of the tactile feedback seemed to be due to the high force magnitude without any texture. Looking at figure 9(c), it is clear that the tendon had a more elastic force profile and the stress increases until breakthrough occurs, with probably little cutting before that point. After the breakthrough, the force drops off rapidly to zero.

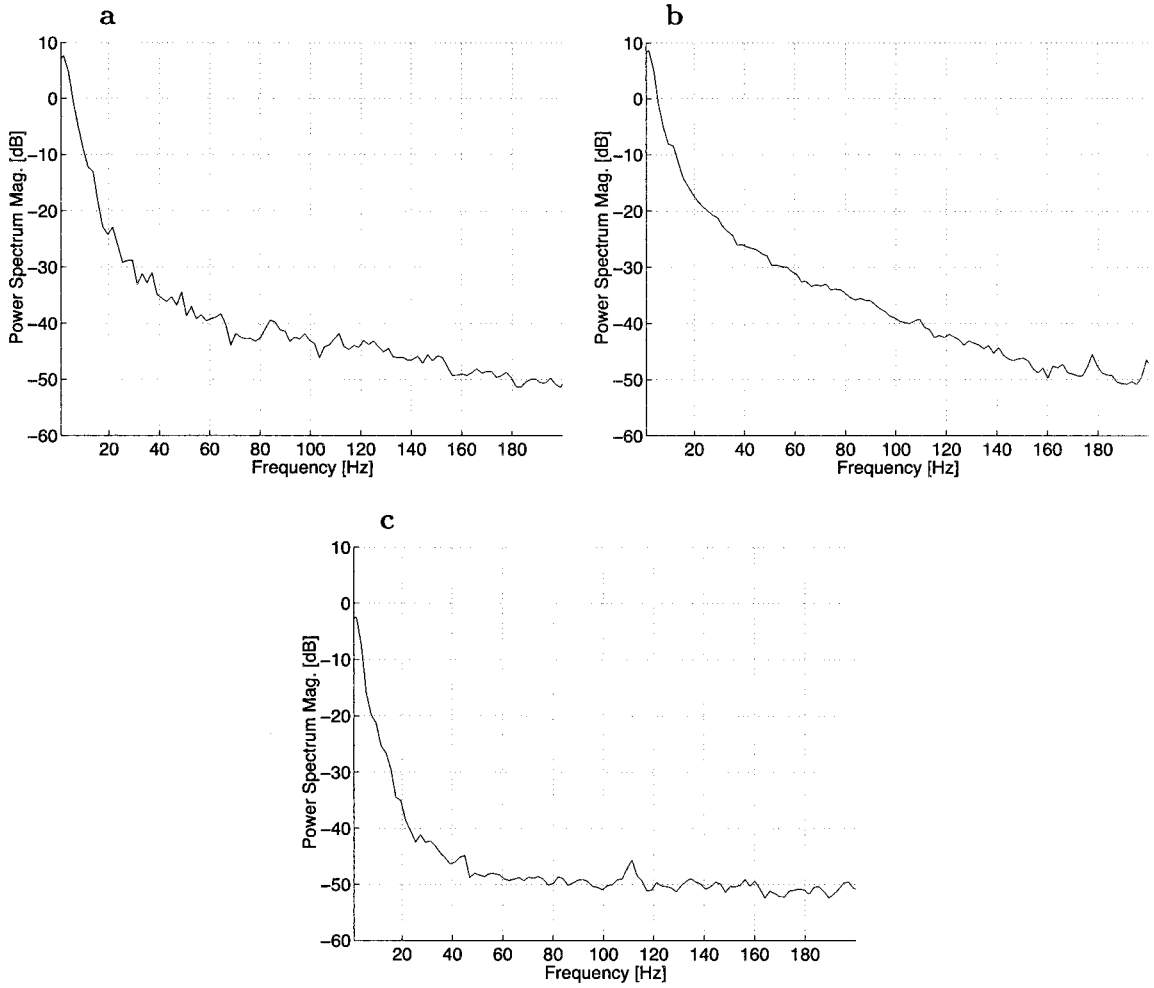

Figure 8. *Comparison of power spectral density curves for the cutting of sheep skin slowly with (surgeon data) (a) Mayo scissors (b) Metzenbaum scissors, and (c) Iris scissors.*

4.4.1 Textural Components. Because some of the tissues expressed little or no magnitude force difference from the blank, the difference felt for these tissues may strictly result from their nonuniformity. Based on the power spectral analysis, textural components were low frequency and hence should perhaps more appropriately be expressed in deg^{-1} rather than Hertz. In other words, the question whether the synthesis of textural components should be done temporally rather than spatially is unresolved.

To see whether these components could explain the differences in feel for other samples, the results from the sheep experiments were investigated for the same tissues. (See figure 10.)

One difference that stands out is that for the sheep: the muscle cut seemed smoother than the liver cut, whereas this relationship was opposite for the rat tissues. This could be a result of the fact that the sheep liver is much larger and actually engulfs the scissors in the tissue as they cut through it, enhancing textural components. The sheep skin was similar to the rat skin; however, it naturally had a considerably larger force magnitude component (18 N versus 8 N). The sheep tendon, like the rat tendon, displayed a behav-

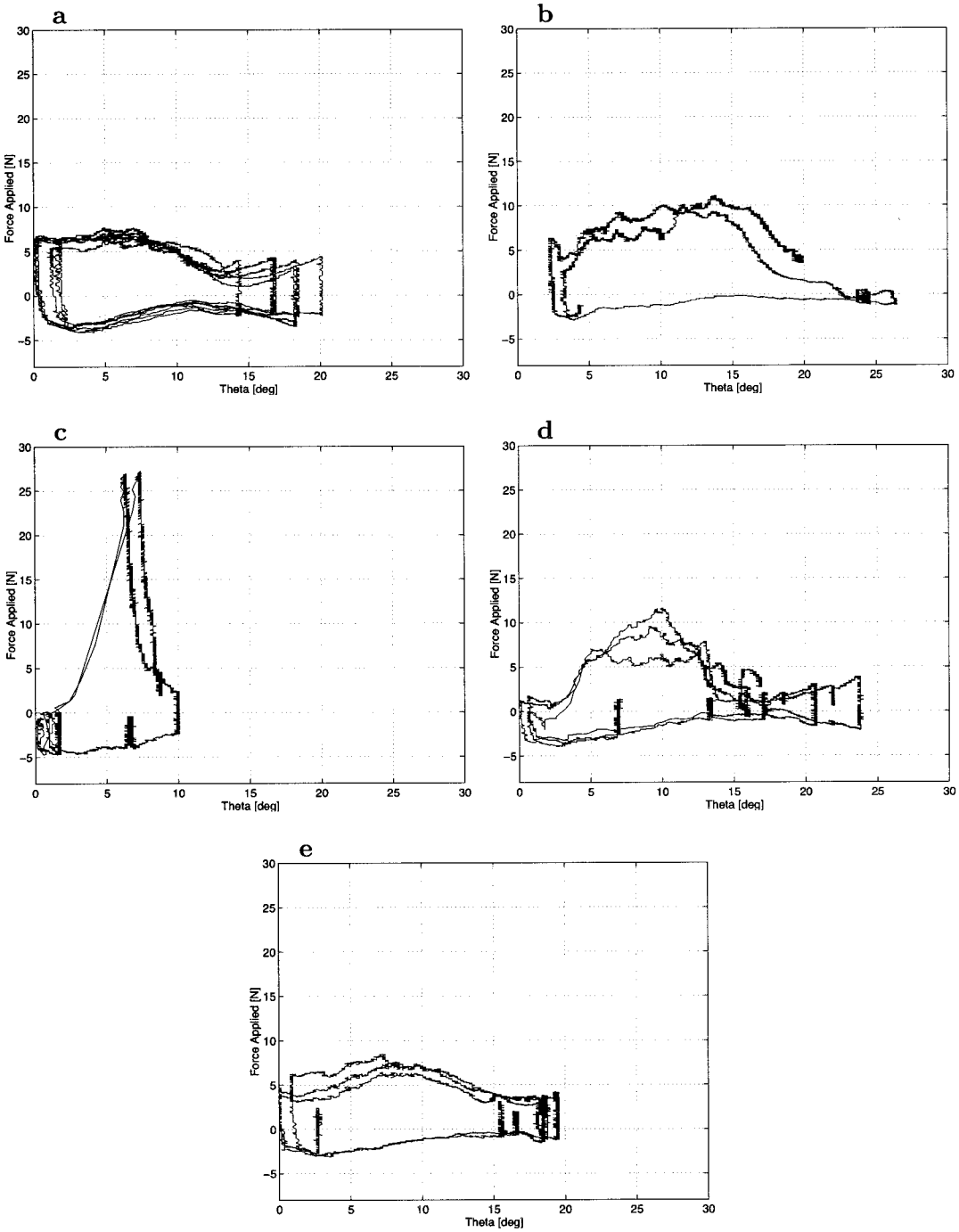

Figure 9. *Comparison of curves for different rat tissue cuts made with the Mayo scissors (surgeon data). (a) blank, (b) muscle, (c) tendon, (d) skin, and (e) liver.*

ior in which the stress increases to a large value until breakthrough. Some of the tissues like the skin and tendon had a similar texture between the rat and sheep for the Mayo scissors. We now compare the Metzenbaum cutting of rat tissues by looking at figure 11.

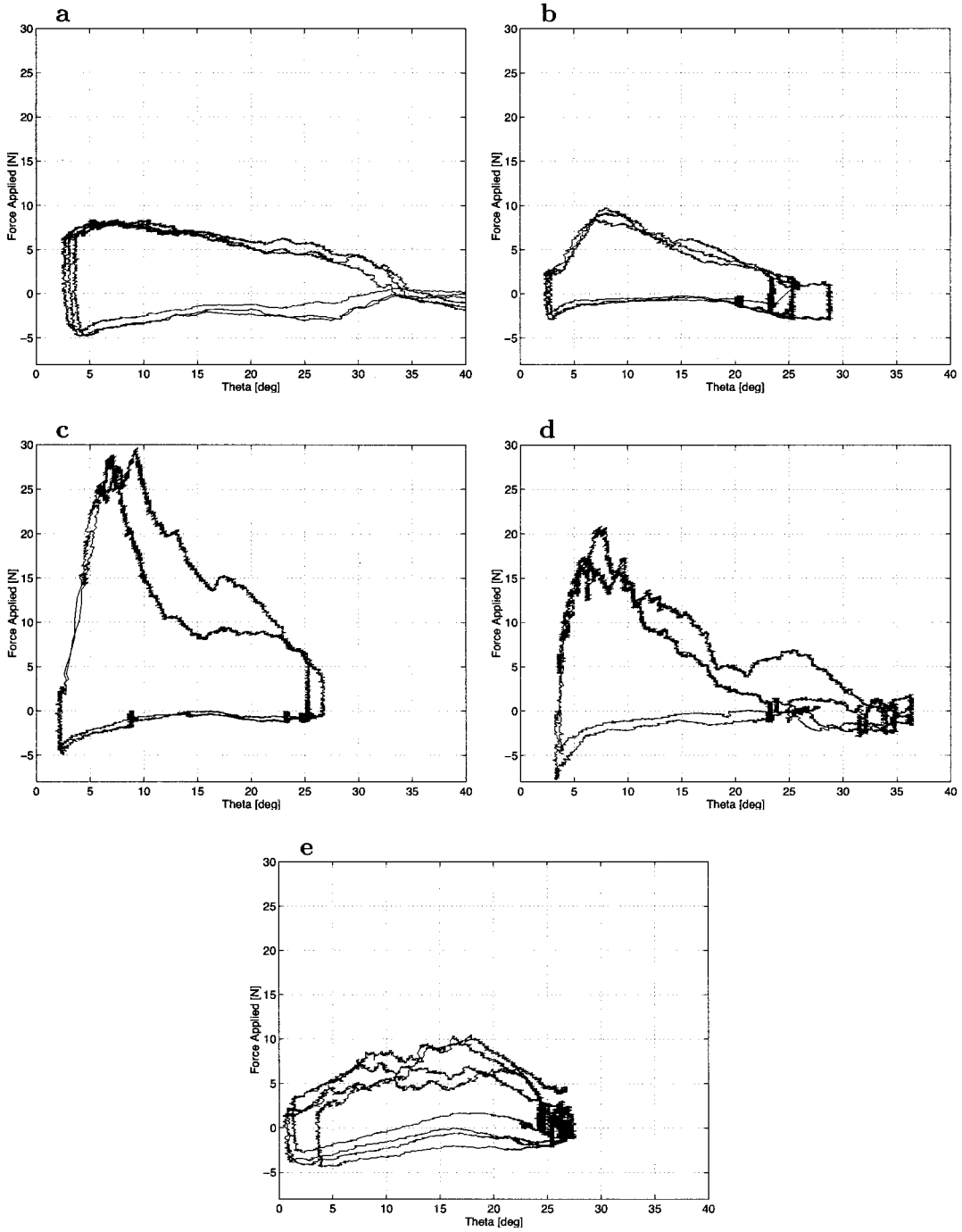

Figure 10. *Comparison of curves for different sheep tissue cuts made with the Mayo scissors (surgeon data). (a) blank, (b) muscle, (c) tendon, (d) skin, and (e) liver.*

The same trends were visible for the Metzenbaum cutting of rat tissues as for the Mayo scissors. The blank for the Metzenbaum scissors was relatively smooth, as is the liver cut. The tendon cut also involved a steep rise in the force until breakthrough, displaying the same elastic behavior. Furthermore,

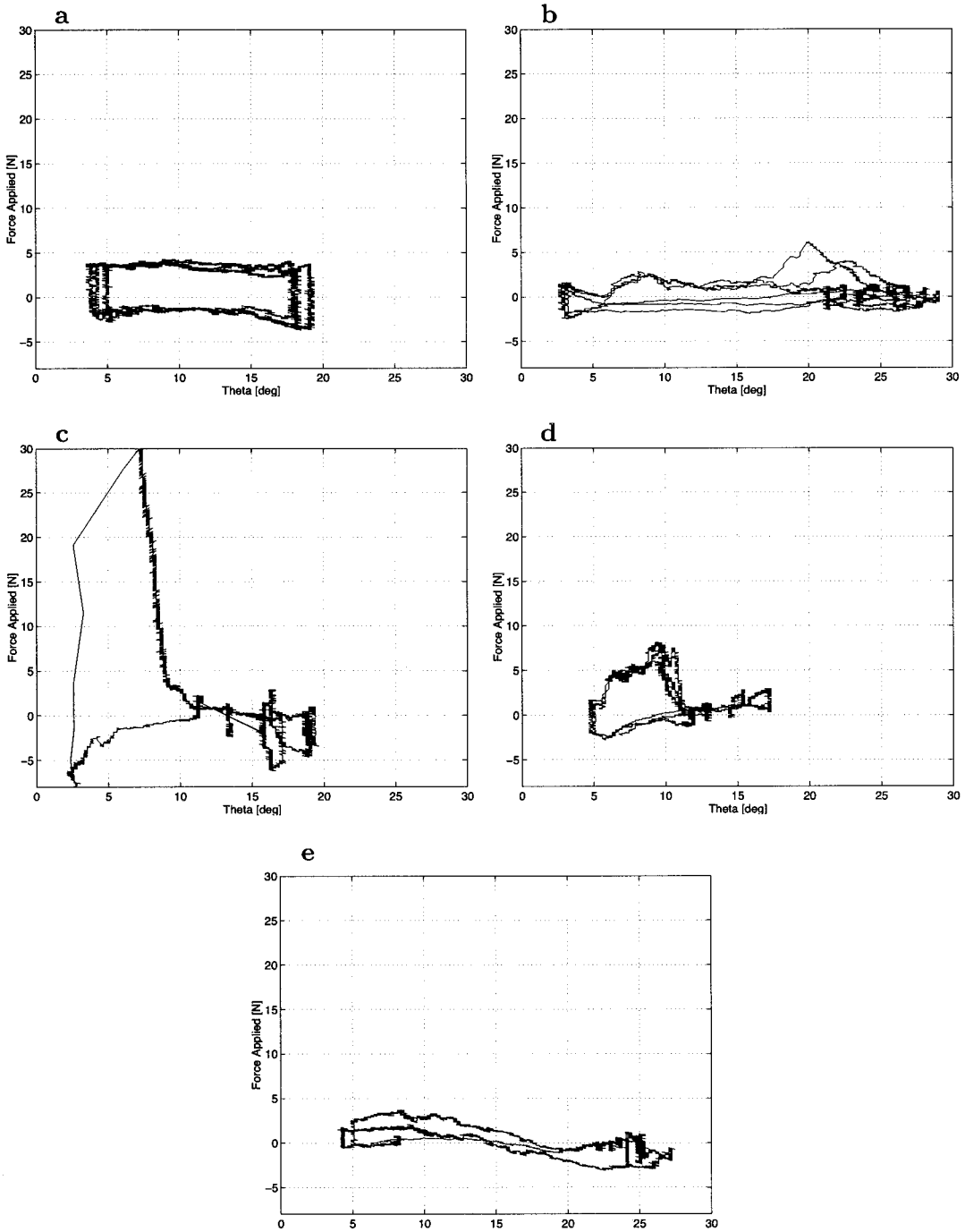

Figure 11. *Comparison of curves for different rat tissue cuts made with the Metzenbaum scissors (surgeon data). (a) blank, (b) muscle, (c) tendon, (d) skin, and (e) liver.*

the skin and muscle cuts with the Metzenbaum contained textures similar to the ones obtained with the Mayo scissors.

Although all of these sheep tissue trials were available for the Metzenbaum scissors, some comparisons are still possible. For the cutting of sheep skin with the Metzen-

baum scissors, a behavior similar to that of sheep skin cut with the Mayo scissors could be seen. The fast cutting of fascia with the Metzenbaum and the sheep liver cut closely resemble the Mayo cuts. As with the Mayo, the magnitudes for cutting the sheep tissues are much larger when compared to the rat tissues. For example, the force to cut skin for sheep is 20 N versus 6 N for the rat skin. As for the Mayo scissors, the liver for the sheep was more textured than the rat liver and required a larger force: 7 N versus 2 N.

In summary, it seems that the differences in haptic sensations resulted from a combination of varying textural components and magnitude force differences. These textures were not high frequency because approximately 99% of the power is in the frequency components below 5 Hz.

4.5 Effect of Velocity

To test the influence of the velocity θ on the force, experiments were performed at two speeds, fast and slow, which were determined by the surgeon while cutting. As mentioned, it was found that slow corresponded to a speed smaller than 15 deg./sec. with an average of 7 deg./sec. and fast to a speed greater than 15 deg./sec. with an average of 44 deg./sec. The average speeds depended on the material being cut. For example, the average fast speed for the blank runs was greater than 100 deg./sec. whereas the average fast speed for cutting skin was 25 deg./sec.

To determine whether the results were significantly different between the two speeds, another sum of squares analysis was used to determine the variability in the slow runs, SSE_S, the fast runs, SSE_F, and the variability between the average slow and fast runs, SSE_{S-F}. Again, entire curves were compared point by point along θ because no accurate model for the closing curve exists.

The results of the SSE analysis are presented in table 3. There did not seem to be a statistically significant difference between the slow and fast cutting speeds for any of the Mayo and Metzenbaum experiments, but the Iris scissors gave a different result. The fast versus slow speed registered as significantly different for the sheep skin cut longitudinally, the rat skin cut longitudinally, the rat liver, and the sheep muscle. It seems premature to draw concrete conclusions about the invariance of the force measure with respect to velocity, except in the case perhaps of the more sensitive Iris scissors.

5 Pilot Study of Cutting Simulations

The "haptic recording" approach was used to create cutting simulations. A custom-designed haptic device was developed to mimic Metzenbaum scissor handles, and three cutting tasks (rat skin, liver, and tendon) and one blank condition could be displayed. Despite the present limitations of the data and of the hardware, it is shown that realistic simulations are possible.

Two preliminary experiments were conducted to examine the effectiveness of virtual simulations of scissor cutting. The first examined the realism provided by a custom-designed haptic display by comparing it to real Metzenbaum scissors. The second experiment examined the performance of subjects while indentifying various tissues using haptic feedback alone. Their performance was assessed both during real and virtual cutting replaying selected haptic recordings. Quantitative and qualitative feedback indicated that the simulations were effective at simulating the haptic experience of cutting biological tissues.

5.1 Apparatus and Data Preparation

The haptic device consisted of a pair of Metzenbaum scissor arms: one stationary and the other attached to a wheel driven by a motor by a frictionless transmission of ratio 3.5:1, as shown at the top of figure 12. The system includes the device, a power amplifier, computer interface boards, and a control computer, as shown in figure 13. The actuator used was a Maxon RE 25 mm dia./20 W motor, with an HP HEDS 5540 encoder. Calibration of the angle between the scissor arms yielded a resolution of 0.053 deg. A PWM amplifier (25A-series, Model 12A8) from Advanced Motion Control was used. A Servo To Go card (Model 2) was used to read the encoders, and a Measurement Computing card (CIO-DAS 1600/12) was used to provide D/A.

Table 3. *Comparing Fast and Slow Cutting Speeds (Surgeon Data)*

Scissor	Tissue	Max (SSE_F, SSE_S)	SSE_{S-F}	Statistically different?
Mayo	Blank	1.6	1.1	N
	Skin (sheep, L)	6.0	1.7	N
	Skin (sheep, T)	2.5	1.6	N
	Skin (rat, L)	2.2	0.8	N
	Skin (rat, T)	1.2	0.9	N
	Fascia (sheep)	1.5	1.4	N
	Liver (rat)	1.2	0.8	N
Metz	Blank	1.1	0.9	N
	Skin (sheep, L)	4.9	3.0	N
	Skin (sheep, T)	6.3	4.9	N
	Skin (rat, L)	2.6	1.2	N
	Liver (rat)	1.3	0.6	N
Iris	Blank	2.0	1.2	N
	Skin (sheep, L)	7.8	9.6	Y
	Skin (rat, L)	6.5	5.2	N
	Skin (rat, T)	5.1	5.7	Y
	Fascia (sheep)	6.5	4.5	N
	Liver (rat)	4.1	0.9	Y
	Muscle (sheep)	4.5	10.9	Y

The computer had a Pentium III 800 MHz processor. A multithreaded control program displayed graphics at 50 Hz and haptics at 1 KHz.

While selecting the force profiles suitable for cutting simulations, it was observed that the forces differed widely, depending on the controlled variables of tissue type, animal type, and scissor type. We selected the Metzenbaum scissors and rat tissues because the forces were generally lower, thereby decreasing the possibility of clipping the force signal. The data collected from empty scissors and three tissues (liver, skin, and tendon) were used. Each data set shown in figure 14 displays several cuts, resulting in overlapping curves. Recall that, when surgeons cut, a repetitive motion is used that never closes fully the scissors.

Before the data could be replayed for simulation, it was first segmented as described in subsection 3.4. Using these raw haptic recordings would not yield a realistic simulation because the subjects could use scissor an-

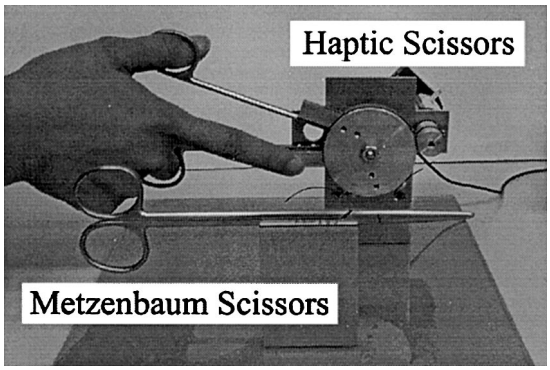

Figure 12. *The haptic scissors and a pair of real Metzenbaum scissors are mounted on a stationary platform.*

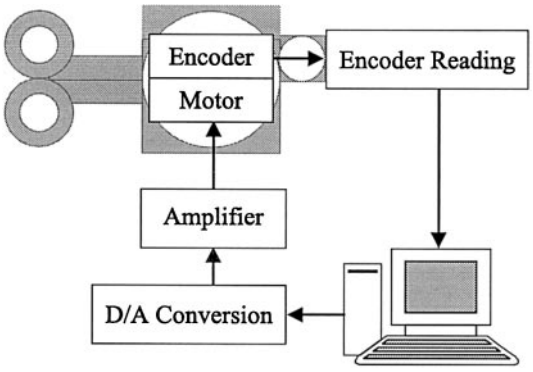

Figure 13. *The haptic system consists of the haptic device, an amplifier, computer interface boards, and a control computer.*

gles not contained in the data. Thus, to limit the amount of "fabricated" data outside of the measured angles, we limited the motion to closing only, extracting the closing segment of one data loop for each tissue. This also helped to eliminate the effect of different cutting styles in identification experiments. To provide forces for complete closure of the scissors, the current force trend was maintained from the minimum angle in the data to zero degrees.

Within one segment of the data, there were multiple force measurements for each potentiometer reading. Thus, the force measurements, ranging from one to twenty data points at a single angle, were averaged for each angle. Next, the data were filtered with an exponentially weighted moving average filter to remove noise that felt clearly unnatural in preliminary simulations. The data were then scaled to reflect the correct force at the handles of the scissors, as the original data represented forces at the cutting point between the scissor blades. A final change was also made to lower the tendon forces: the rat used to acquire data had stiffer tendons than any of the rats to which we had access for perceptual experiments. Thus, we lowered the peak force of the tendon simulation significantly. The final data used in simulation are shown overlaid with the original data in figure 14.

Once the simulation data were obtained, a lookup table was created, providing a list of angles and forces with a one-to-one correspondence. If the angle measured by the haptic scissors encoder was between the angles listed in the table, linear interpolation was used to determine the correct force for display. The software enabled the experimenter to choose which simulation data set to display (none, blank, liver, skin, or tendon), as shown in figure 15. This visual display was hidden from the subjects during experiments.

5.2 Methods and Results

5.2.1 Realism of Haptic versus Real Scissors.

In this test, the haptic scissors were programmed to simulate the feel of blank Metzenbaum scissors during closing. Five male subjects, ranging in age from 22 to 38, were selected with the criterion that they had no previous knowledge of the haptic scissors nor of the purpose of the test. They also had no previous experience with surgical or haptic devices. The subjects were blindfolded and asked to use three pairs of scissors mounted on a stationary platform: the haptic scissors (programmed to reproduce a blank cut) and two pairs of complete Metzenbaum scissors labeled Scissors 1 and 2.

Each subject was informed that there were at least one real pair and at least one simulated pair. After testing each pair by closing the scissor arms only once, the subjects had to decide whether each of the three scissors were real or simulated. One pair of the real Metzenbaum scissors had never been used before (Scissors 1), resulting in a slightly different feel from the other pair of real scissors which had been previously used for cutting rat tissues and cleaned (Scissors 2).

All subjects reported that the Scissors 1 were real, but only 60% thought that the Scissors 2 were real. Forty percent of the subjects judged that the haptic scissors were real. In other words, the haptic scissors were sometimes judged to be real, but some subjects also thought that the real scissors were artificial.

A likely reason why the haptic scissors did not feel real was that they did not reproduce the correct behavior of the blades near 0 deg. because, we did not have data in this angle range to use as a haptic recording. An important comment was that the haptic scissors and the smoother pair of Metzenbaum scissors felt very similar. Another observation was that real scissors of the same

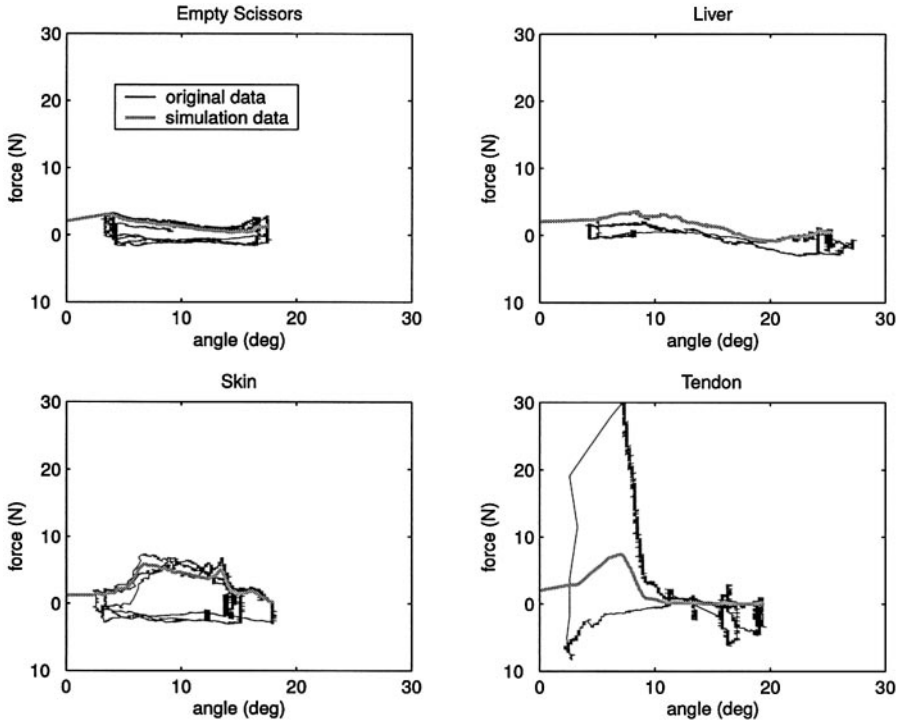

Figure 14. *Data used for haptic simulations. The simulation data uses filtered data from one closing of the scissors over rat tissues or blank. It is represented in the figure as a thick gray line.*

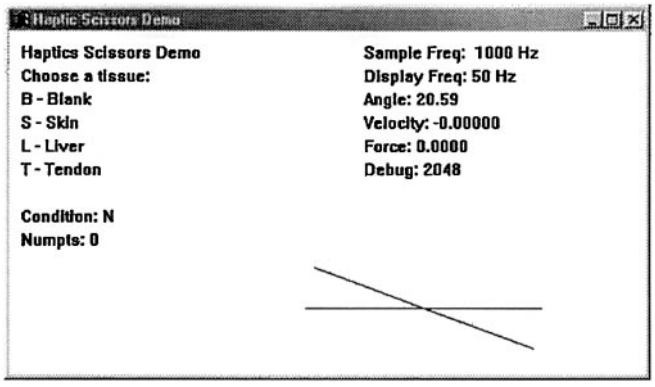

Figure 15. *Visual display for the haptic scissors.*

type could feel significantly different from each other. In this case, the increased force in the second pair was due to the fact that they had been used and washed, which probably increased friction in the joint.

5.2.2 Identification of Real and Virtual Tissues.

In the second experiment, subjects cut real and virtual rat tissues with real Metzenbaum or simulated scissors and attempted to identify tissue types by haptic feedback alone. These tissues were by necessity from animals different from those used for the initial data gathering.

During phase I, the subjects first visually inspected the prepared animals and made several cuts in each tissue with a pair of Metzenbaum scissors: in liver, skin, and tendon. They also tried blank cuts. Then, each subject was blindfolded and proceeded to make blind cuts in blocks of four cases presented in a randomized order. The samples were held between the blades of the mounted scissors by a surgical assistant who also controlled the quality of the cut. The subjects were informed that there was one sample of each tissue in each block. Their task was to label the four cases by feel alone. They were allowed to repeat some cuts to make a

Table 4. *Experimental Results for Matching Tissue Types to Real and Virtual Tissues*

	Real Tissues (Phase I)					Virtual Tissues (Phase II)				
Subject	Blank	Liver	Skin	Tendon	Correct	Blank	Liver	Skin	Tendon	Correct
1	S	B	L	T	1	B	L	T	S	2
2	L	B	S	T	2	S	B	L	T	1
3	B	L	T	S	2	L	B	S	T	2
4	B	L	S	T	4	L	B	S	T	2
5	B	S	L	T	2	Did not perform experiment				
6	B	L	T	S	2	Did not perform experiment				

decision and to relabel them until they felt confidence in their judgment.

During phase II, the subjects repeated the tissue identification with the virtual tissues, approximately one week after they tested the real tissues in phase I. Of the six subjects participating in phase I, four were available for phase II. Because of the limitations of the record and replay approach (as further discussed in subsection 5.3), subjects were limited to experience haptic feedback during closing only, but could repeat the closing action several times as in phase I. The only difference is that subjects were asked to limit the scissors opening to the largest angle for which we had data.

Fifty-four percent of the subject tissue identifications were correct for real tissues (phase I). For virtual tissues (phase II), the percentage of correct identifications was 44%. Results are shown in table 4. It was expected that the matching would be better with the real tissues. However, the low success rates show that subjects in general are not good at matching tissues by feel alone. The t-value for comparing the means in the real and virtual environments was 0.62 (eight degrees of freedom, p-value = 0.29), so we conclude that the difference is not statistically significant. That is, subjects did not perform significantly worse with the virtual tissues than with the real tissues, but this could be due to the limited data from this pilot study.

Qualitative feedback also indicated that completely realistic tissue display is not necessary to convince subjects of the "realism" of virtual environments involving cutting. However, as several subjects commented after the experiments, removal of acoustic noise from the motor, forces when opening the scissors, and translational motion of the scissors while cutting are necessary for a true sense of "immersion" in a virtual environment.

5.3 Discussion

Rendering simplicity is the main advantage of haptic recordings. A lookup table is all that is needed for real-time haptic display. Any other data manipulation, such as filtering and scaling, can be performed as a preprocessing step. In general, subjective responses in the experiments indicated that the haptic simulations felt realistic, although not "exactly like" the real rat tissues.

Yet, there are several limitations to using haptic recordings. First, appropriate display of the recorded haptic data required that we modify the original data significantly. Filtering, scaling, and fabricating data for "empty" angles were required to create simulations that could be compared against real tissues. It is hard to determine the precise amount or type of filtering, scaling, or additional data that should be used without more detailed empirical modeling. Because these factors were determined "by feel" by the experimenter, a certain amount of arbitrariness was injected into the final simulation, although we used direct haptic recordings.

In addition, we had to limit the subjects to a single closing of the scissors. Although the data were recorded

in loops of opening and closing, an even larger amount of fabricated data would have been needed to simulate these loops. The stationary mounting limited the simulation to the closing action. If subjects were to perform continuous cutting motions, it would be more natural to move the scissors forward. This could be accomplished by mounting the scissors on a translational haptic device or on a haptic device that was designed for having this capability (Hayward et al., 1998).

A final limitation is that a haptic recording is essentially a snapshot of the "feel" for one particular tissue at one instance. Depending on the history of the tissues measured, the data may not reflect the average tissue forces. It was clear from our experiments that the tendon forces of the comparison rats were much lower than those originally measured. Because we scaled a portion of the high forces down to match the available tissues by feel, there was no guarantee that our scaling was perceptually correct. These issues underscore the importance of continued data collection, analysis, and modeling.

Although the authors believe that more complete modeling is the ideal approach, using haptic recordings provided significant insight. Using the direct data, we were able to determine the mechanical and control requirements of the haptic system. We were also able to verify that realistic simulations were indeed possible, at least in some cases, before embarking on a lengthy modeling procedure.

6 Conclusions

The forces involved in the cutting of tissues for three surgical scissors were acquired and analyzed. Although the experimental method allowed for the determination of general trends in the data, exact quantitative measures for the forces required to cut tissues remain indeterminate. Several improvements to the data acquisition method have been identified and proposed. The acquired data were displayed on a specialized haptic interface using the "haptic recording" rendering approach. Although straightforward and computationally efficient, this method lacks the flexibility for surgical simulation. This result motivates the need for further experiments and parameter-based models describing the cutting forces. Equally important is the necessity to pursue careful psychological testing to relate these parameters to the performance of subjects.

6.1 Future Recommendations

Improvements include eliminating the grip effect from future data collection because it partially inhibits the determination of the innate tissue properties. Conversely, this raises the subtle issue that a simulator might need to account for the grip. At least two grip types have been identified, the pull-open and push-closed grips, but others may exist, especially when the scissors are at rest. The surgeon's grip is quite different from that of the student's, which indicates the necessity to involve a trained surgeon in experiments at these early stages (or conversely to use measurements as a performance assessment technique during training).

Larger sample sizes are desirable to average out some of the sources of error and variability between tissue samples. The tissue variability is a result of innate tissue differences from region to region, especially for large tissues such as skin or muscle, and from the varying tissue structures attached to the tissue of interest. Tissue must be prepared carefully to obtain the greatest uniformity possible between runs.

Equally important for the determination of the exact forces to cut tissues is the moisture content of the tissue. This should be controlled for or accounted for. Videotaping and having assistants in the operating room would allow appropriate measure to be taken to control the tissue thickness and the visible differences between tissue samples.

Furthermore, it was determined that the transverse and longitudinal cutting conditions may not be necessary for all of the experimental conditions. Once this result is validated, the cutting direction could be eliminated as a parameter for skin cuts. Limiting the data set is especially important as uniform tissue is difficult to obtain. Further experiments in the cutting directions of other tissues are warranted.

The scissor dynamics themselves are among the factors that influence what the surgeon feels. The length of

the scissor arms determines the mechanical advantage that influences the amount of force the user must apply at the handle. The blade characteristics such as edge sharpness, joint screw tightness, and degree of curvature change the feel of the scissors. For these reasons, it is important to test the scissors before purchasing them and to determine quantifiable metrics for these parameters.

An improvement to the force measurement would be a better rejection of off-axis stresses and thermal effects. This might prove worthwhile in reducing the variability in the data.

6.2 Important Trends

Although the data collection method would benefit from these improvements, several observations are still possible. First, looking at the average maximum force, the measurable difference between tissues include a larger magnitude in the force applied for thicker and stronger tissues. In descending order, forces required to cut the rat tissues were found to be greatest for the tendon, then the muscle, skin, and finally the liver. For the sheep tissues, this order was determined to be tendon, skin, muscle, fascia, and finally liver. Although there is a magnitude force difference between tissues, an equally important difference may be in the textural components of the force versus angle curves. Whereas the liver experiments for the rat and muscle experiments for the sheep are relatively smooth, the skin and fascia curves are more ridged or textured.

This texture consists of only low-frequency signal components because approximately 99% of the signal components are below 5 Hz. Therefore, a simulator may provide realistic haptic interaction with low bandwidth. For the tendon, however, there is no measurable textural components. The force increases until breakthrough after which the force drops off quickly. By comparing two cutting speeds, the force was found to be independent of the cutting rate for the Mayo and Metzenbaum scissors.

Looking into invariants between either tissues or scissors provided the observation that the force resolved at the cutting point required to cut a tissue consistently increases as the scissor angle closes. This can be explained by the amount of deformed tissue due to the change in contact geometry as the scissors close. The response to cutting thus highly depends on the details of tissue deformation and rupture, which in turn both depend on the macro and the micro geometry of the scissor blades. As well, the cutting curve is highly repeatable within a run, even if the cutting incident angle varies, which indicates that the tissue cutting force characteristics can be determined with the measured force and scissor angle alone. These findings are consistent with the cutting model recently introduced by Mahvash and Hayward (2001). Other cutting dynamics identified in the data include the breakthrough angle and the contact area between the blades.

Acknowledgments

At McGill University, initial funding for this research was provided by the project "Haptic Devices for Teleoperation and Virtual Environments" (HMI-6) supported by IRIS (Phase 2), the Institute for Robotics and Intelligent Systems, part of Canada's National Centers of Excellence program (NCE), and an operating grant "High Performance Robotic Devices" from NSERC, the Natural Science and Engineering Council of Canada. Additional funding for this research was provided by an NSERC University/Industry Technology Partnership Grant, McGill/MPBT "A Balanced Haptic Device for Computer/User Interaction."

At Johns Hopkins University, Drs. Homayoun Mozaffari and Romer Geocadin., both of the Johns Hopkins Medical Institutions, were very helpful in conducting experiments with rat tissues. Torrey Bievenour designed the initial prototype of the haptic scissors. Ms. Chial was supported by the NSF Research Experience for Undergraduates Program through The Johns Hopkins University NSF Engineering Research Center for Computer Integrated Surgical Systems and Technology (grant #EEC9731478).

References

Ackerman, M. J. (1994). The visible human project. *Medicine meets virtual reality II: Interaction technology and healthcare*, (pp. 5–7). Amsterdam: IOS Press.

Baumann, R., Maeder, W., Glauser, D., & Clavel, R. (1998). Force feedback for minimally invasive surgery. *Medicine meets virtual reality IV: Interaction technology and healthcare* (pp. 564–579). Amsterdam: IOS Press.

Basdogan C., Ho, C., Srinivasan, M. A., Small, S., & Dawson, S. (1998). Force interactions in laparoscopic simulations: Haptic rendering of soft tissues. *Medicine meets virtual reality IV: Interaction technology and healthcare* (pp. 385–391). Amsterdam: IOS Press.

Basdogan, C., Ho, C.-H., & Srinivasan, M. (1999). Simulation of tissue cutting and bleeding for laparoscopic surgery using auxiliary surfaces. *Medicine meets virtual reality VII* (pp. 38–44). Amsterdam: IOS Press.

Bicchi, A., Canepa, G., De Rossi, D., Iacconi, P., & Scilingo, E. P. (1996). A sensorized minimally invasive surgical tool for detecting tissutal elastic properties. *Proceedings of the IEEE Int. Conf. on Robotics and Automation,* 884–888.

Biesler, D., & Gross, M. H. (2000). Interactive simulation of surgical cuts. *Proceedings of IEEE Pacific Graphics 2000,* 116–125.

Brower, I., Ustin, J., Bentley, L., Sherman, A., Dhruv, N., & Tendick, F. (2001). Measuring in vivo animal soft tissue properties for haptic modeling in surgical simulation. *Medicine Meets Virtual Reality 2001* (pp. 69–79). Amsterdam: IOS Press.

Carter, F. J., Frank, T. G., Davies, P. J., & Cuschieri, A. (2000). Puncture forces of solid organ surfaces. *Surg. Endosc., 14*(9), 783–786.

Delp, S., Loan, P., Basdogan, C., & Rosen, J. (1997). Surgical simulation: An emerging technology for training in emergency medicine. *Presence: Teleoperators and Virtual Environments, 6*(2), 147–159.

Duck, F. A. (1990). *Physical properties of tissue: A comprehensive reference book*. London: Academy Press.

Green, P. S., Jensen, J. F., Hill, J. W., & Shah, A. (1993). *Mobile telepresence surgery* (Tech. Rep.). SRI International.

Hannaford, B., Trujillo, J., Sinanan, M., Moreyra, M., Rosen, J., Brown, J., Lueshke, R., & MacFarlane, M. (1998). Computerized endoscopic surgical grasper. *Medicine meets virtual reality IV: Interaction technology and healthcare* (pp. 265–271). Amsterdam: IOS Press.

Hayward, V., Gregorio, P., Astley, O., Greenish, S., Doyon, M., Lessard, L., McDougall, J., Sinclair, I., Boelen, S., Chen, X., Demers, J.-P., Poulin, J., Benguigui, I., Almey, N., Makuc, B., & Zhang, X. (1998). Freedom-7: A high fidelity seven axis haptic device with application to surgical training. Experimental robotics V. In Casals, A., de Almeida, A. T. (Eds.), *Lecture Notes in Control and Information Science*, vol. *232,* (pp. 445–456). New York: Springer-Verlag.

Hirota, K., Tanaka, A., & Kaneko, T. (1999). Representation of force in cutting operation. *Proceedings of IEEE Virtual Reality,* p. 77.

Hunter, I., Jones, L., Sagar, M., Lafontaine, S., & Hunter, P. (1995). Ophthalmic microsurgical robot and associated virtual environments. *Computers in Biology and Medicine, 25*(2), 173–182.

Kuppersmith, R. B., Johnston, R., Jones, S. B., & Herman A. J. (1996). Virtual reality surgical simulation and otolaryngology. *Arch. Otolaryngol. Head Neck Surg., 122,* 1297–1297.

Longnion, J., Rosen, J., Sinanan, M., & Hannaford, B. (2001). Effects of geared motor characteristics on tactile perception of tissue stiffness. *Medicine Meets Virtual Reality 2001* (pp. 286–292). Amsterdam: IOS Press.

MacFarlane, M., Rosen, J., Hannaford, B., Pellegrini, C., & Sinanan, M. (1999). Force feedback endoscopic grasper helps restore the sense of touch in minimally invasive surgery. *Journal of Gastrointestinal Surgery, 3,* 278–285.

MacLean, K. (1996). The "Haptic Camera": A technique for characterizing and playing back haptic properties of real environments. *Proceedings of ASME Dynamic Systems and Control Division, 58,* 459–467.

Mahvash, M., & Hayward, V. (2001). Haptic rendering of cutting: A fracture mechanics approach. *Haptics-e: The Electronic Journal of Haptics Research, 2,*3 [Available on-line: www.haptics-e.org].

Mann, P. S. (1998). *Introductory statistics,* 3rd ed. New York: John Wiley & Sons.

Okamura, A. M., Dennerlein, J. T., & Howe, R. D. (1998). Vibration feedback models for virtual environments. *Proceedings of the IEEE International Conference on Robotics and Automation, 1,* 674–679.

Okamura, A. M., Hage, M. W., Dennerlein, J. T., & Cutkosky, M. R. (2000). Improving reality-based models for vibration feedback. *Proceedings of the ASME Dynamic Systems and Control Division, 69,* 1117–1124.

Ottensmeyer, M. P., & Salisbury, J. K. (2001). In vivo data acquisition instrument for solid organ mechanical property measurement. In *MICCAI 2001,* LNCS 2208 (pp. 975–982). New York: Springer-Verlag.

Pai, D. K., Lang, J., Lloyd, J. E., & Woodham, R. J. (2000). ACME: A telerobotic active measurement facility. In P. Corke and J. Trevelyan (Eds.), *Experimental Robotics VI:*

Lecture Notes in control and information sciences, 250. (pp. 391–400). New York: Springer-Verlag.

Picinbono, G., Delingette, H., & Ayache, N. (2000). Nonlinear and anisotropic elastic soft tissue models for medical simulation. *Proceedings of the IEEE International Conference on Robotics and Automation,* 1370–1375.

Richard, C., Cutkosky, M. R., & MacLean, K. (1999). Friction identification for haptic display. *Proceedings of the ASME Dynamic Systems and Control Division, 67,* 327–334.

Richmond, J. L., & Pai, D. K. (2000). Active measurement and modeling of contact sounds. *Proceedings of the IEEE International Conference on Robotics and Automation,* 2146–2152.

Rosen, J., Hannaford, B., MacFarlane, M., & Sinanan, M. (1999). Force controlled and teleoperated endoscopic grasper for minimally invasive surgery: Experimental performance evaluation. *IEEE Transactions on Biomedical Engineering, 46,* 1212–1221.

Satava, R. M. (1996). Advanced simulation technologies for surgical education. *Bull. A. Coll. Surg., 81*(7), 77–81.

Satava, R. M., & Jones, S. B. (1997). Virtual environments for medical training and education. *Presence: Teleoperators and Virtual Environments, 6*(2), 139–146.

Vuskovic, V., Kauer, M., Szekely, G., & Reidy, M. (2002). Realistic force feedback for virtual reality based diagnostic surgery simulators. *Proceedings of the IEEE International Conference on Robotics and Automation,* 1592–1598.